Three-Dimensional Simulation of Gaseous Fuel Injection Through a Hybrid Approach

L. Andreassi

A. L. Facci

Department of Mechanical Engineering,
University of Rome Tor Vergata,
Rome, 00133 Italy

S. Ubertini
Engineering Faculty,
Department of Technology,
University of Naples, 'Parthenope',
Naples, 80100, Italy

Direct injection of gaseous fuel has emerged to be a high potential strategy to tackle both environmental and fuel economy requirements. However, since the electronic gaseous injection technology is rather new for automotive applications, limited experience exists on the optimum configuration of the injection system and the combustion chamber. To facilitate the development of these applications computer models are being developed to simulate gaseous injection, air entrainment, and the ensuing combustion. This paper introduces a new method for modeling the injection process of gaseous fuels in multidimensional simulations. The proposed model allows holding down grid requirements, thus, making it compatible with the three-dimensional simulation of an internal combustion engine. [DOI: 10.1115/1.4000288]

1 Introduction

The task of capturing the evolution of a transient jet with a fully 3D modeling is rather complicated due to intense grid requirements. Namely, in a typical automotive thermal engine, the injector diameter is about 1/100 of the characteristic dimension of the combustion chamber and the injector orifice surface must be divided into many computational cells in order to investigate the jet evolution. Although a detailed numerical three-dimensional simulation of the gas injection phase could be performed [1], its computational cost makes it not suitable to be coupled with a detailed multidimensional simulation of the whole internal combustion engine, where further phases are simulated (i.e., combustion, valve and piston motion, gas exchange process, etc.). Therefore simplified models are required because of their effectiveness in providing accurate information while maintaining acceptable computational times.

2 Injection Model

The model described in this paper has been thought to correctly predict the gas jet evolution while holding down grid requirements. The jet is described with an original methodology based on the integration of a phenomenological model and a fully three-dimensional simulation performed with a modified version of the KIVA 3V code developed in the last decade by our research group [2–7].

Manuscript received May 13, 2009; final manuscript received July 7, 2009; published online April 16, 2010. Editor: Dilip R. Ballal.

2.1 Quasi-steady Jet. Many experimental evidences show that a transient gas jet can be described as composed of two different regions [8,9], as follows:

1. a semi spherical shaped vorticous region on the tip of the jet;
2. a quasi-steady conical region feeding the vortex structure in terms of mass, momentum, and energy.

As the aim of the zero-dimensional model is capturing the evolution of the first part of the jet, the interest is focused on the description of the conical and quasi-steady regions. The evolution of the vortex structure and thus the estimation of the jet tip penetration is left to the 3D detailed simulations.

Making the hypothesis that the jet evolves into a constant pressure environment and considering that outside the injector there is no length scale imposed, it is possible to state that velocity and concentration profiles are self-similar. It means that nondimensional fields do not depend on the distance form the orifice. This condition can be expressed as

$$\frac{U}{U_m} = f\left(\frac{r}{\delta}\right), \quad \frac{x}{x_m} = g\left(\frac{r}{\delta}\right) \tag{1}$$

where δ is a dimension representative of the jet width. Assuming $\delta = r_{1/2}$, where $r_{1/2}$ is the radius where the velocity is a half of the axial velocity (half velocity radius) and combining Eq. (1) with the momentum conservation, the jet shape and velocity profile along the jet axis can be calculated as

$$\frac{r_{1/2}}{z + z_0} = a, \quad \frac{U_m}{U_0} = b\frac{r_0}{z + z_0 - z_{\text{core}}} \tag{2}$$

The second term in Eq. (2) takes also into account the existence of the so-called *potential core* located nearby the nozzle, with an almost uniform mean velocity. We assume that the core region length is influenced only by the length scale imposed by the injector diameter as $z_{\text{core}} = Cd_0$, where C is a model constant to be tuned in the updating phase. According to [8], local velocity and concentration are calculated as a function of axial values

$$\frac{U}{U_m} = e^{-\alpha\xi^2}, \quad \frac{x}{x_m} = \sqrt{\frac{U}{U_m}} = e^{-1/2\alpha\xi^2} \tag{3}$$

where $\alpha = ln(2)$ and $\xi = r/r_{1/2}$.

The density profile along the jet axis can be determined from the steady-state condition, which means that the injected gas mass flow inside the jet must be constant on any surface along the jet axis. The mass flux can be expressed as

$$\dot{m} = \int_s x\rho U dS \tag{4}$$

so that, integrated together with Eqs. (3), takes to

$$x_m = \dot{m}\frac{3\alpha}{2\pi r_{1/2}^2 \rho U_m (1 - e^{-3/2\alpha(R/r_{1/2})^2})} \tag{5}$$

2.1.1 Inflow Conditions. In automotive engines injection pressure is high enough to produce a sonic and underexpanded jet. As a consequence, it suddenly expands just outside the orifice thanks to a complicated system of shock waves. This process has been described with a simplified model based on the following hypotheses:

1. negligible air entrainment during the expansion process;
2. sonic flow both at the orifice and at the Mach disk;
3. constant temperature during the expansion process; and
4. the expansion process is isoentropic.

As the expansion region is very small compared with jet penetration, it may be assumed that the underexpanded jet behaves as

Table 1 Injection properties

	Subsonic	Supersonic
Injector diameter	1.6 mm	0.6 mm
Relative injection pressure	10 kPa	150 bars
Injection temperature	298 K	298 K
Environment pressure	1 bar	30 bars
Environment temperature	298 K	298 K
Reynolds number	5000	115,000

a correctly expanded one originating from a larger area or pseudo-area. The pseudo-area can be then related to the real one as

$$\frac{A_e}{A_n} = Cd\frac{P_0}{P_e}\left(\frac{2}{k+1}\right)^{k/k-1} \tag{6}$$

2.1.2 Numerical Scheme Implementation. The coupling between the phenomenological model and the three-dimensional code is performed by supplying, at every time-step, the concentration and velocity values in the computational cells inside a control volume containing the jet. A dedicated subroutine is used to find out the cells that are included within the stationary region of the jet and to calculate the velocity and concentration values. However, a control volume larger than the stationary region cone is employed in order to prevent excessive diffusion in the first part of the jet, as observed in other models [10], and guarantee overall mass conservation, as the injected gas diffusing outside the cone would not be taken into account.

The model parameters that have to be evaluated and updated are as follows:

Table 2 Injection model main parameters

Parameter	a	b	C
Value	0.5	5.28	9

1. the constant values a, z_{core}, and z_0 to be evaluated according to experimental data;
2. the constant b to be calculated through momentum conservation equations;
3. the switch criteria between the simplified model and the 3D simulation (i.e., jet penetration).

3 Model Updating and Validation

The proposed numerical model is validated by comparing our numerical results with experimental data found in literature [9,10] in both subsonic and supersonic conditions. The main properties of the injection process are summarized in Table 1. The computational domain is a brick volume of dimension $8\times8\times25$ cm divided into 120,000 nodes. The employed nonuniform mesh is refined close to the nozzle, with a minimum cell dimension equal to a quarter of the injector diameter. The value of the model constants employed for the present simulation are listed in Table 2.

Numerical and experimental penetration lengths are compared in Fig. 1. This quantitative comparison confirms the good agreement between numerical and experimental results in particular for the subsonic case. In the supersonic case the agreement is still very good, especially in the first 1 ms time window, with a jet penetration slightly lower than 6 cm. Then the code underestimates the jet penetration with respect to experimental data. However, it is important to note that the 3D model starts when the jet penetration is about 0.7 cm and therefore the higher deceleration of the numerical jet should be attributed to the three-dimensional fluid dynamics simulation. It is also noticeable that model tuning parameters have not been changed between the two validation tests. This is consistent with the observation [11] that the spreading rate and the velocity decay of a turbulent free jet are independent of the Reynolds number, which is the only significant nondimensional parameter for a round free jet. Furthermore, velocity decay constant (b) that have been used for these tests is similar of the experimental value that can be found in [11].

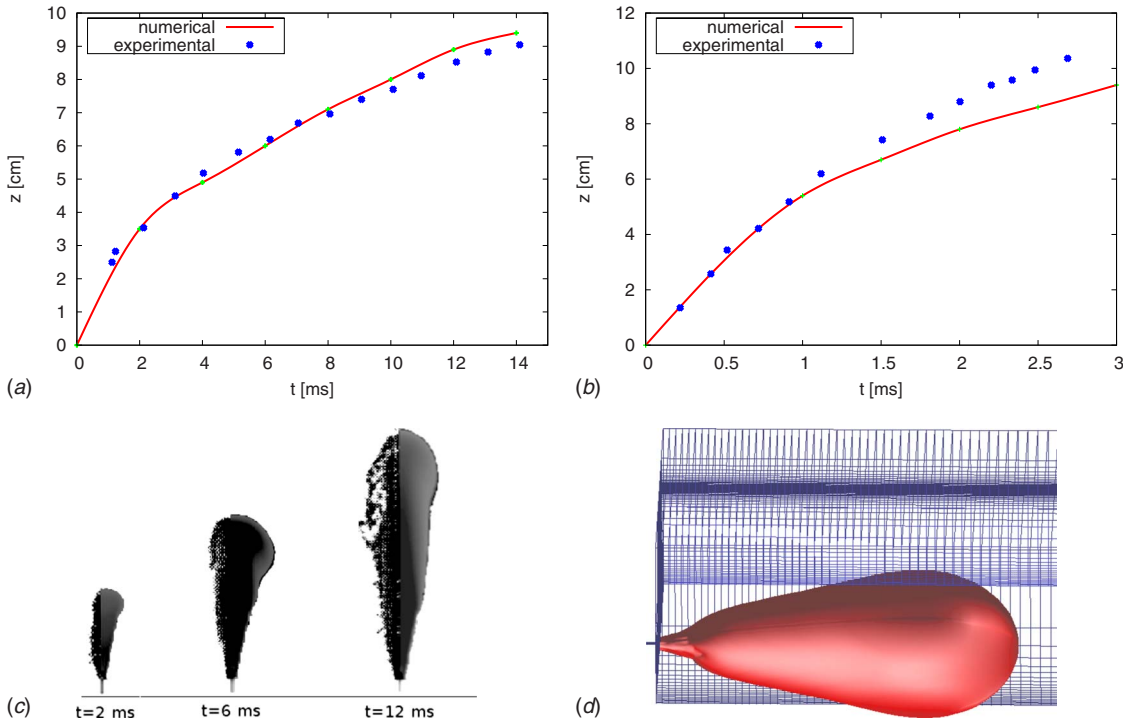

Fig. 1 Comparison between numerical and experimental penetrations for a subsonic jet: (*a*) subsonic, (*b*) supersonic, (*c*) experimental and numerical jet shapes, and (*d*) 3D jet shape

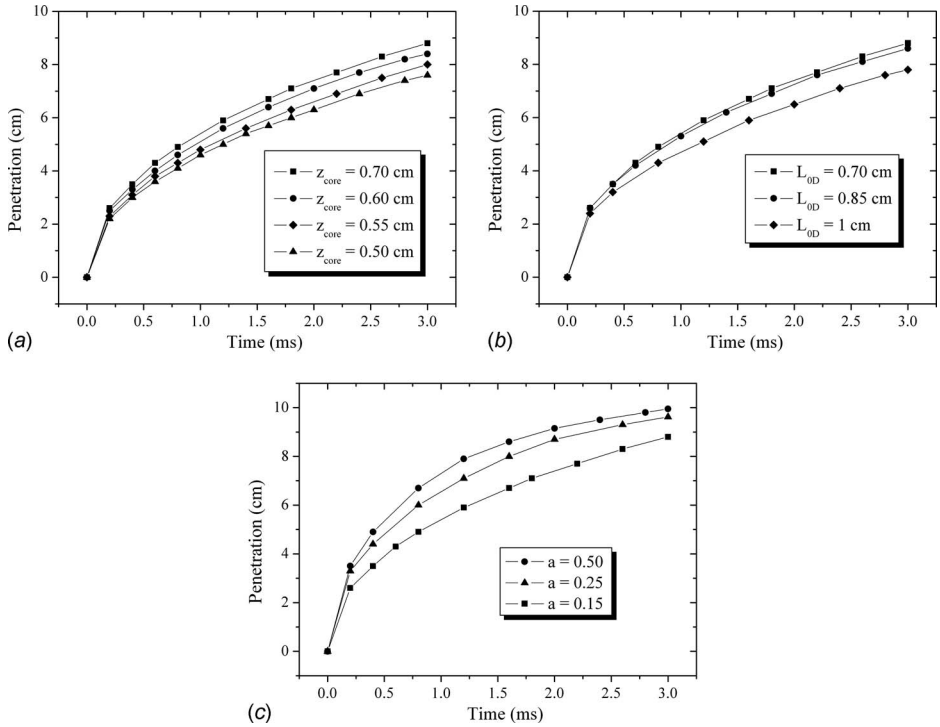

Fig. 2 Sensitivity analysis results: (*a*) influence of z_{core}, (*b*) influence of the 0D model length, and (*c*) influence of *a*

4 Sensitivity Analysis

In order to complete the model validation and allow a better comprehension of its behavior, a sensitivity analysis on model parameters is presented here. The main parameters that have been taken into account are as follows:

1. the length of the core region z_{core};
2. the length of the phenomenological described region;
3. the jet spreading rate (i.e., constant a).

Figure 2(*b*) shows the influence of the switch criteria between the phenomenological model and the three-dimensional simulation. This is a key point on the correct implementation of the present model, as the dimension of the region described by the phenomenological model (L_{0D}) affects the accuracy of the calculation and the mesh size. With regard to this aspect, it is remarkable that the influence of this parameter correctly tends to saturation decreasing the phenomenological region dimension.

Figure 2(*a*) shows how sensitive the model is to changes in the length of the potential core region, where the flow is almost uniform, and no mixing occurs. As expected, the longer is the core region, the higher is the jet penetration, as the velocity decay starts after the core region length. It is worth pointing out that this parameter has an important influence on jet penetration and that it is the main tuning parameter of the phenomenological model.

Jet penetrations with different values of the model constant a are reported in Fig. 2(*c*). As a is a measure of the jet spreading rate, its value has a significant influence on penetration. As observed in [11] and in Sec. 3, a should be almost invariable for turbulent fully developed free jets in a wide range of Reynolds numbers. Therefore, it should be updated once and then it should remain constant at varying operating conditions.

5 Conclusions

This paper presents a hybrid numerical approach to simulate gaseous fuel direct injection in internal combustion engines. The very first part of the jet evolution is described through a phenomenological model. After a prescribed penetration length, the fluid dynamics is left to the three-dimensional code. This procedure allows to keep simultaneously acceptable grid size limitations and to be effective in describing the jet evolution in terms of both penetration and shape. The model has been validated at two injection pressures (i.e., 1.1 bar and 180 bars) corresponding to a subsonic and a sonic and underexpanded jet. A sensitivity analysis is also performed to show the effects of the model constants on the dynamic behavior of the jet. The numerical investigation points out the importance of the core region for what concerns the evolution of the first part of the jet, and how to determine it in the updating phase.

Acknowledgment

This research is partially supported by the Italian Ministry of Instruction, University, and Research within the project FIRB 2007 "Studio, progettazione e sviluppo e sperimentazione di nua nuova generazione competitiva di motori innovativi a basso consumo ed a basso impatto ambientale nell'arco dell'intero ciclo di vita."

Nomenclature

Subscripts and Superscripts

0 = nozzle
a = environment
e = equivalent
m = jet axis
s = stagnation

Symbols

a, b, C = model constants
k = isoentropic exponent
$\dot{m}$ = mass flow (kg/s)
p = pressure (Pa)
r = radius (m)
R = jet radius (m)

$r_{1/2}$ = half-velocity radius (m)
T = temperature (K)
U = velocity (m/s)
x = concentration
A = area (m^2)
z = jet penetration axis (m)
z_{core} = core region length
z_0 = apparent jet origin position
α = ln(2)
δ = characteristic jet dimension (m)
ξ = nondimensional velocity profile
ρ = density (kg/m^3)

References

[1] Baratta, M., Catania, A. E., Spessa, E., Hermann, L., and Roessler, K., 2008, "Multi Dimensional Modelling of Direct Natural-Gas Injection and Mixture Formation in a Stratified Charge SI Engine With Centrally Mounted Injector," SAE Technical Paper No. 2008-01-0975.

[2] Andreassi, L., Cordiner, S., Mulone, V., Reynolds, C. C. O., and Evans, R. L., 2005, "The Effect of Varying the Injected Charge Stoichiometry in a Partially Stratified Charge Natural Gas Engine," SAE Technical Paper No. 2005-01-0247.

[3] Andreassi, L., Cordiner, S., Mulone, V., Reynolds, C. C. O., and Evans, R. L., 2005, "A Mixed Numerical-Experimental Analysis for the Development of a Partially Stratified Compressed Natural Gas Engine," SAE Technical Paper No. 2005-24-029.

[4] Bozza, F., Gimelli, A., Andreassi, L., Rocco, V., and Scarcelli, R., 2008, "1D-3D Analysis of the Scavenging and Combustion Process in a Gasoline and Natural-Gas Fuelled Two-Stroke Engine," SAE Technical Paper No. 2008-01-1087.

[5] Andreassi, L., Ubertini, S., and Allocca, L., 2007, "Experimental and Numerical Analysis of High Pressure Diesel Spray-Wall Interaction," Int. J. Multiphase Flow, **33**, pp. 742–765.

[6] Allocca, L., Andreassi, L., and Ubertini, S., 2007, "Enhanced Splash Models for High Pressure Diesel Spray," ASME J. Eng. Gas Turbines Power, **129**(2), pp. 609–621.

[7] Andreassi, L., Cordiner, S., Mulone, V., Reynolds, C., and Evans, R., 2004, "Numerical-Experimental Comparison of the Performance of a Partially Stratified Charge Natural Gas Fuelled Engine," ASME Paper No. ICEF-2004-912.

[8] Ouelette, P., and Hill, P. G., 1992, "Visualization of Natural Gas Injection for a Compression Ignition Engine," SAE Technical Paper No. 921555.

[9] Fujimoto, H., Hyun, G.-S., Nogami, M., Hirakawa, K., Asai, T., and Senda, J., 1997, "Characteristics of Free and Impinging Gas Jets by Means of Image Processing," SAE Technical Paper No. 970045.

[10] Papageorgakis, G., and Assanis, D. N., 1998, "Optimizing Gaseous Fuel Air-Mixing in Direct Injection Engine Using an RNG Based $k-\epsilon$ Model," SAE Technical Paper No. 980135.

[11] Pope, S., 2000, *Tubulent Flows*, Cambridge University Press, Cambridge.